2016 23rd Iranian Conference on Biomedical Engineering and 2016 1st International Iranian Conference on Biomedical Engineering (ICBME), Amirkabir University of Technology, Tehran, Iran, 23-25 November 2016

A Real-Time Stable Volumetric Mass-Spring Model Based on a Multi-Scale Mesh Representation

An Application to Medical Virtual Reality

Sepide Farhang, Amir Hossein Foruzan*
Biomedical EngineeringDepartment, Faculty of Engineering, Shahed University, Tehran, Iran.
s.farhang@shahed.ac.ir, a.foruzan@shahed.ac.ir

Yen-Wei Chen
Intelligent Image Processing Lab, College of Information Science and Engineering, Ritsumeikan University, Japan.
chen@ritsumei.ac.jp

***Abstract*—Representation of soft tissues in virtual reality environments has been focused by researchers with applications including training medical students and surgeons, treatment planning, monitoring and telesurgery. A major challenge of current modeling schemes such as Boundary Element, Finite Element, and Mass-Spring Models is to deal with volume preserving. Another challenge is the complexity of a model which results in a more realistic visualization; however, it increases computational cost. In this paper, we propose a Mass-Spring model to represent liver volume. It contains a series of multi-scale surface meshes with interconnections between the models and therefore it is considered as a volumetric mesh model. To preserve the volume of the gland, an external force is transmitted from the surface to internal meshes. By designing a specific data structure to hold coordinates of mesh points, we are able to render mesh movement in nearly real-time using conventional CPU architectures. Localization of the external force is adjusted by the penetration depth parameter. Qualitative evaluation of the results revealed the promising performance of the proposed model. The stability of our Mass-Spring model under large deformation is another novelty of our method too.**

Keywords: Medical virtual reality, Mass-spring model, Liver surgical simulator, volumetric mesh, Multi-scale mesh model.

I. INTRODUCTION

Medical virtual reality has been the focus of research in recent years. Typical applications include treatment planning, training of medical students and surgeons and telesurgery. In laparoscopic surgery, as an example, a camera is inserted into the body through a small hole which helps a physician to perform a minimally invasive surgery. Main advantages of this type of surgery are short hospital stay, decreasing the trauma risk and patient pains after surgery. However, there are some limitation including degraded visual information and losing direct tactile. Pre-operative training can help physicians to adapt to this new type of conditions.

Surgical simulators provide a virtual reality by which a surgeon can learn how to coordinate his eyes/hands in a 2D monitor. Moreover, they give a virtual environment to perform surgery before applying on a patient which efficiently prevents destructive outcome. Fast and accurate visualization of an organ is a prerequisite of a medical virtual reality system.

II. PREVIOUS WORKS

Several methods have been proposed to represent both rigid and non-rigid human tissues [1, 2]. Two complete reviews of these researches are papers by Meier *et al.* [3] and Nealen*et al* . [4]. Visualization of a soft tissue is more complex and requires high computational cost due to its dynamic behavior and tool-tissue interactions. A tissue is represented by a model which can be deformed by user interaction and is therefore called a deformable model.

Deformable model techniques are classified into two groups : (1) continuum mechanics approaches and (2) discrete models. The first class includes Finite Element/Boundary Element Methods (FEM/BEM) [5, 6]. The discrete model category contains deformable splines [7], mass-spring [8], linked volume [9] and chain-mail models [10].

FEM is one of the common numerical approaches to solve Partial Differential Equations (PDEs). In FEM, a tissue is considered as a continuous connected volume and is discretized into a finite number of discrete parts. Any global deformation is applied locally in each part. Using true material parameters based on biomechanics experiments (i.e. Poisson Ratio and Young's Modulus), the mechanical behavior of a FEM-based model is more realistic. However, the computational cost of the model is more expensive and it is therefore not suitable for interactive applications. Another deficiency of the model is its low accuracy for large deformations. Several researchers proposed techniques to speed up conventional FEM; however, it is still considered as a complex algorithm [11-13].

BEM is a method which is closely related to FEM; however, the surface of an object (instead of its volume) is discretized and represented by a mesh. Therefore, 3D computations are reduced to 2D computations which make the whole process faster. The BEM technique cannot be used to

978-1-5090-3452-9/16/$31.00 ©2016 IEEE

model inhomogeneous tissues and is not used to represent viscous or damping effects.

As a type of discrete models, deformable splines were the first deformable models that were applied to the field of surgery simulations [7]. These models represented the surface of an object by a set of spline functions. Corresponding to a spline function, there are some control points to change the shape of the object. Computation complexity and reduced realism were two major factors to make these models obsolete [3].

A Mass-Spring Model (MSM) utilizes discrete mass points (nodal network) and massless springs together with dampers as connections to create a surface mesh. Deformation is performed by the dynamics of the mass points and springs. Accurate parameters tuning and a proper time step affect realistic dynamical behavior and stable results respectively. This model is the fastest method to develop a real-time simulator; however, it is not as accurate as BEM/FEM models. The MSM model has been largely used to represent surfaces of objects. When a force is applied on the surface of the object, the surface will deform; however, the volume of the object will not be preserved. Several researchers have been improved the model efficiency by introducing hybrid models [14,15] or enhancing the basic structure to increase its accuracy [16-19].

In this paper, we proposed a volumetric mass-spring model to represent hepatic tissue. The innovations of our method include volume preservation by introducing a multi-scale MSM model and real-time performance using a novel data structure. Preserving the volume of an object makes visualization more realistic. An external force applied on the surface of liver is penetrated vertically and transversally. The computational efficiency is comparable to a single mesh model too. Our model is stable under large deformations which is superior to conventional MSM models too.

III. PROPOSED METHOD

The pipeline of our method is shown in Figure 1. It consists of two major steps: (1) Initialization and (2) processing user-interactions. Initialization includes reading input binary image, representation of the input volume by mesh and pre-computing several multi-dimensional matrices. Employing the multi-dimensional matrices is a novelty in our method which increases the speed of our code and removes the need to high performance computers. Rendering consists of surface mesh processing, generating volumetric mass-spring model and visualization.

A. Initialization

After segmentation of a liver in the input CT image, the binary volume is represented by a triangulated mesh structure. The mesh data include vertices and surfaces which are computed by the Marching cube algorithm. The coordinates of the mesh points are stored in an $N \times 3$ matrix where N is the number of mesh vertices. We build a two scale mesh model by shrinking the input volume and constructing a new mesh model. The new mesh is smaller than the initial surface and is put inside the larger one. Therefore, we model inside the liver by another surface mesh.

A user can decide on the penetration depth and locality of an external force. Locality means how far an external force can affect nearby points. Based on the parameters that are selected by the user, we construct a multi-dimensional matrix which includes hierarchical neighbourhood information of each point in several levels.

Assuming the locality parameter is set to 3. When an external force is applied to the surface of liver, the collision vertex is detected and the multi-dimensional matrix is initialized (Figure 2a). The indices of the collision point together with all its neighbours and the neighbours of the 2nd to 3rd levels are stored in the hierarchical data structure (Figure 2b). There is a trade-off between locality and computational cost.

When an input force is applied to the surface of the liver, an attenuated version of the force will be applied to the both sides of the internal mesh and later it will be applied to the opposite side of the external mesh too. By introducing this technique, a visualized object is not considered as a hollow volume anymore and its volume is preserved. Therefore, a single external force produces three other external forces which are applied on internal surface meshes (Figure 3). Corresponding to each collision point, a hierarchical structure is built. Inclusion of internal layers is aimed to produce an effect similar to FEM with lower complexity.

B. Processing User-interctions

To check for the collision between instrument's tip and the tissue surface, the differences between the instrument's tip position and all node positions are calculated for the outer-most layer.

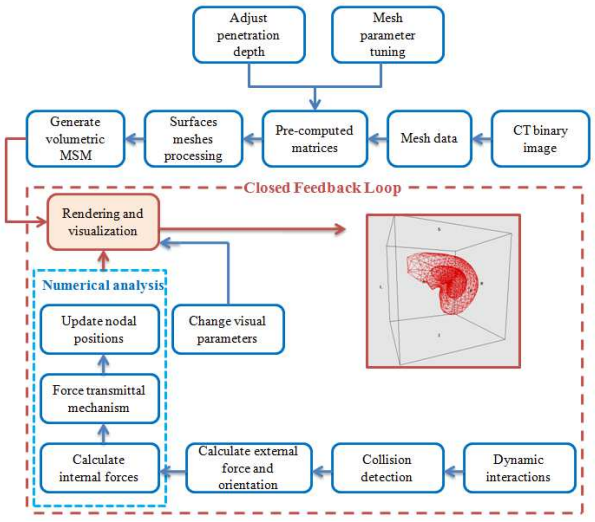

Figure 1. The pipeline of the proposed method.

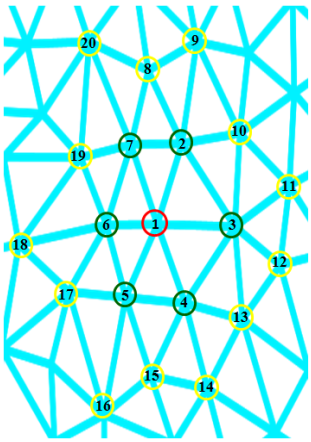

(a)

Level/ pixel index	Effective Neihbours
0/1	2, 3, 4, 5, 6, 7
1/2	1, 3, 7, 8, 9, 10
1/3	1, 2, 4, 10-13
1/4	1, 3, 5, 13-15
1/5	1, 4, 6, 15-17
1/6	1, 5, 7, 17-19
1/7	1, 2, 6, 19, 20, 8
2/8	2, 7, 9, 20
2/9	2, 8, 10
2/10	2, 3, 9, 11
2/11	3, 10, 12
2/12	3, 11, 13
2/13	3, 4, 12, 13
2/14	4, 13, 15
2/15	4, 5, 14, 16
2/16	5, 15, 17
2/17	5, 6, 16, 18
2/18	6, 17, 19
2/19	6, 7, 18, 20
2/20	7, 8, 19

(b)

Figure 2. (a) A typical mesh with an external force which is applied to vertex no. 1. (b) The proposed hierarchical structure to hold neighbourhood information of the collision region.

If the distance between the nearest node and the instrument is lower than as specified threshold, a collision will be detected.

Figure 3 represents a typical multi-layer triangular mesh. A is the outer-most layer that an external force is applied on it. In Figure 3, the penetration depth parameter is set to 4. The external force is applied on L_0 , then algorithm create the secondary force to the next layer that is less than the initial force, likewise a few percent of the force is reduced in each layer.

When an external force is applied on the model, the absolute value and direction of the force are calculated. The absolute value of the force is proportional to amount of mouse movement. An attenuated version of the force is also applied to underlying mesh layers. In each layer, the collision point is the minimum distance to the force.

To propagate force through nearby points, we employ Breadth First Search (BFS) algorithm. The node in direct contact with external force is in level L_0 and all neighbours of this node are in level L_1 (Figure 2). This sequence continues to the last level L_{N-1} where N is the locality parameter. The vertices of each level are processed one-by-one until no vertex is remained. Corresponding to each vertex, a flag is defined so that no vertex is processed twice.

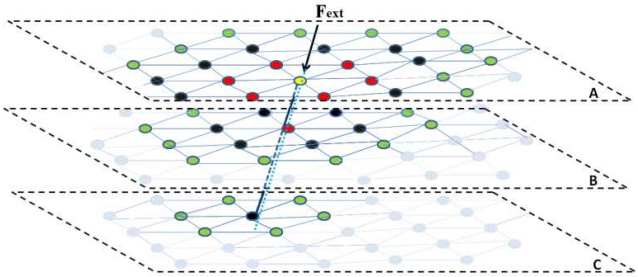

Figure 3. The mechanism used to transmit force to underlying layers. External force is initially applied to the yellow point (L_0). The light blue dotted line represents the force direction. Red, black and green points are collision points in layers L_1 , L_2 and L_3 respectively.

C. *The Mass-Spring Model*

Using Newtonian law of motion, the dynamics of nodes in a Mass-Spring network can be described as (1)

$$M\ddot{X} + \Gamma\dot{X} + \mathrm{K}X = \mathrm{F} \tag{1}$$

In (1), M, Γ, K, X and F are mass, damping coefficient, stiffness, position matrices and external force respectively. On this network there are three types of forces: external, internal and damping forces. External force is applied through user interaction. An internal force is generated by springs connecting nodes together. It tries to return any deformation caused by external force to its initial state. According to Hooke's Law, the spring force matrix (F_s) for linear elastic springs in a network with N nodes is defined as in (2), (3)

$$F_s = K\,\Delta X \tag{2}$$

$$K = \begin{bmatrix} k_0^0 & \cdots & k_{N_i}^0 \\ \vdots & \ddots & \vdots \\ k_0^N & \cdots & k_{N_i}^N \end{bmatrix} \tag{3}$$

In (2), ΔX is the spring length change matrix and N_i is the number of nodes adjacent to the node i. In a Mass Spring model for a single node i equation (2) is rewritten as (4).

$$f_{int}^i = \sum_{j\in N_i} K_j^i \frac{|r^j - r^i| - |r^j - r^i|^0}{|r^j - r^i|}(r^j - r^i) \tag{4}$$

In (4), r is position vector, $|r^j - r^i|$ and $|r^j - r^i|^0$ are current and initial length of spring connecting nodes i and j. The damping force in (1) is velocity-dependent and it represents the viscosity properties. We assume a homogenous tissue and the viscous friction coefficient and stiffness matrices are reduced to a scalar. Therefore, we have a constant scalar stiffness k and a damping coefficient γ for the network and for a single node i, equation (1) is simplified as (5)

$$m^i \frac{d^2 r^i}{dt^2} + \gamma \frac{dr^i}{dt} + f_{int}^i = f_{ext}^i \tag{5}$$

A popular method to numerically solve the second order ordinary differential equation in (5) is the Euler method. We use a backward approach to solve (5) as is shown in (6)-(8).

$$v = \frac{dr}{dt} \tag{6}$$

$$\frac{dv}{dt} = \frac{d^2r}{dt^2} \tag{7}$$

$$v^t = dt * f(v,t) + v^{t-dt} \tag{8}$$

In (8), v^t, v^{t-h} are current and last node velocity respectively, $f(v,t)$ is velocity derivative and dt represents the time step.

An appropriate time step is needed to get stable results. Very small values of *dt* result in low convergence rates and large values make the results oscillating.

Mechanical properties of materials are described by constants called Poisson Ratio and Young's Modulus. The parameters in a mass-spring model have no direct relation with these constants. To achieve a realistic behavior experienced by surgeons, these parameters are estimated by trial and error.

By solving the differential equation in (5), the positions of all displaced nodes are obtained for each time step. This process continues until the difference of position vectors in two consecutive time steps are lower than a threshold.

IV. RESULTS

We employed our method to visualize liver volume in CT images. The penetration depth was set to 4. We used a 2-scale model to preserve the volume. The surface of a liver is represented by 1284 mesh points. We implemented our code on a personal computer with an Intel Core i5 processor with 4 GB of dynamic RAM without any graphics acceleration. The code was implemented in visual studio using OpenGL graphics library.

In Figure 4, variations of a typical point are shown for different values of damping coefficients. Increasing damping coefficient results in reducing the oscillation time. Regarding the stiffness, increasing the parameter restricts final displacement of a node and increases oscillation too. The optimal time step was obtained as *dt*=0.01 so that the algorithm converges in nearly real time and no oscillation occurs.

In Figure 5, snapshots of deformation of a typical model consisting of 1284 nodes and 2560 faces. Black points represent where external forces were applied on the model. As can be seen in Figure 5, a large deformation was applied on the model; however, the model was stable and finally converged.

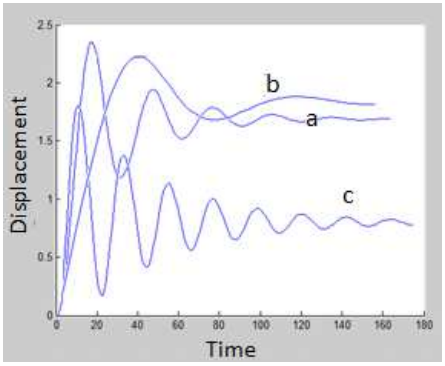

Figure 4. variations of a typical point for different values of tissue parameters. (a) γ=3,K=3 (b) γ=5,K=3 (c) γ=3,K=6.

The effect of localization degree and convergence threshold is illustrated in Figure 5. Computation time increases with threshold, but it grew faster with respect to localization parameter. By increasing convergence threshold from 1e-4 to 1e-3, the computation time is reduced by approximately 44% for a localization of five. In Figure 5, initialization means preparing pre-computed matrices and rendering the volumetric mesh.

Several experiments were performed to find optimum locality parameter and the parameter was selected as 4. Steps of manipulating a typical liver are shown in Figure 6.

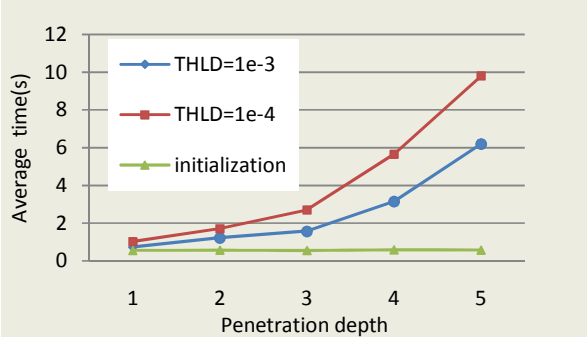

Figure 5. Effect of convergence threshold and degree of localization on the deformation applied computation time.

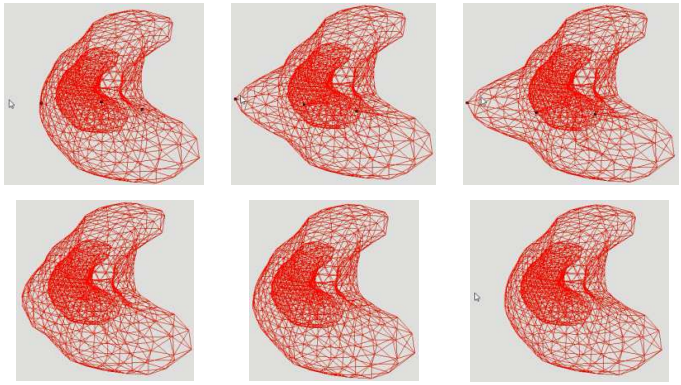

Figure 6. From left to right and top to bottom, snapshots of deformation of a typical model consisting of 1284 nodes and 2560 faces. Black points represent where external forces were applied on the model.

V. DISCUSSION

In this paper we proposed a new method to represent volumetric MSM to preserve an organ volume. The main advantages of our model compared to the other models are volume preservation, real time performance and portability of the code with regard to the algorithm hyper-parameters. In the proposed model, the external force is transferred along surface and depth of a model by setting the penetration depth parameter. Therefore, local or global deformations are represented in this model. We also concerned the stability of the model under large deformations.

VI. FUTURE WORKS

In future, we plan to extend our method so multiple external forces can be applied on different regions. We plan to develop a user-friendly GUI to interact easily with the application too.

REFERENCES

[1] Lin, Yanping, Xudong Wang, Fule Wu, Xiaojun Chen, Chengtao Wang, and Guofang Shen. "Development and validation of a surgical training simulator with haptic feedback for learning bone-sawing skill." Journal of biomedical informatics 48 (2014): 122-129.

[2] Cotin, Stéphane, Hervé Delingette, and Nicholas Ayache. "Real-time elastic deformations of soft tissues for surgery simulation." Visualization and Computer Graphics, IEEE Transactions on 5, no. 1 (1999): 62-73.

[3] Meier, Ullrich, Oscar López, Carlos Monserrat, Mari C. Juan, and M. Alcaniz. "Real-time deformable models for surgery simulation: a survey." Computer methods and programs in biomedicine 77, no. 3 (2005): 183-197.

[4] Nealen, Andrew, Matthias Müller, Richard Keiser, Eddy Boxerman, and Mark Carlson. "Physically based deformable models in computer graphics." InComputer graphics forum, vol. 25, no. 4, pp. 809-836. Blackwell Publishing Ltd, 2006.

[5] Bro-Nielsen, Morten. "Finite element modeling in surgery simulation."Proceedings of the IEEE 86, no. 3 (1998): 490-503.

[6] James, Doug L., and Dinesh K. Pai. "ArtDefo: accurate real time deformable objects." In Proceedings of the 26th annual conference on Computer graphics and interactive techniques, pp. 65-72. ACM Press/Addison-Wesley Publishing Co., 1999.

[7] Cover, Steven A., Norberto F. Ezquerra, James F. O'Brien, Richard Rowe, Thomas Gadacz, and Ellen Palm. "Interactively deformable models for surgery simulation." Computer Graphics and Applications, IEEE 13, no. 6 (1993): 68-75.

[8] Teschner, Matthias, Bruno Heidelberger, Matthias Müller, and Markus Gross. "A versatile and robust model for geometrically complex deformable solids." In Computer Graphics International, 2004. Proceedings, pp. 312-319. IEEE, 2004.

[9] Jansson, Johan, and Joris SM Vergeest. "A discrete mechanics model for deformable bodies." Computer-Aided Design 34, no. 12 (2002): 913-928.

[10] Gibson, Sarah F. "3D chainmail: a fast algorithm for deforming volumetric objects." In Proceedings of the 1997 symposium on Interactive 3D graphics, pp. 149-ff. ACM, 1997.

[11] Gabbert, U., H. Berger, J. Grochla, H. Koppe, and C. Willberg. "A real time simulator for virtual surgery." COMEC10 (2010).

[12] Fu, Y. B., and C. K. Chui. "Modelling and simulation of porcine liver tissue indentation using finite element method and uniaxial stress–strain data."Journal of biomechanics 47, no. 10 (2014): 2430-2435.

[13] Goulette, François, and Zhuo-Wei Chen. "Fast computation of soft tissue deformations in real-time simulation with Hyper-Elastic Mass Links."Computer Methods in Applied Mechanics and Engineering 295 (2015): 18-38.

[14] Xu, Shaoping, Xiaoping Liu, and Hua Zhang. "Simulation of soft tissue using mass-spring model with simulated annealing optimization." In Automation and Logistics, 2009. ICAL'09. IEEE International Conference on, pp. 1543-1547. IEEE, 2009.

[15] Zhu, Bo, and Lixu Gu. "A hybrid deformable model for real-time surgical simulation." Computerized Medical Imaging and Graphics 36, no. 5 (2012): 356-365.

[16] del-Castillo, Esteban, Luis Basañez, and Ernest Gil. "Modeling non-linear viscoelastic behavior under large deformations." International Journal of Non-Linear Mechanics 57 (2013): 154-162.

[17] Sulaiman, Salina, Abdullah Bade, and Siti Hasnah Tanalol. "Surgical simulation using Mass-Spring model variant." (2011).

[18] San-Vicente, Gaizka, Iker Aguinaga, and Juan Tomás Celigüeta. "Cubical mass-spring model design based on a tensile deformation test and nonlinear material model." Visualization and Computer Graphics, IEEE Transactions on 18, no. 2 (2012): 228-241.

[19] Basafa, Ehsan, and Farzam Farahmand. "Real-time simulation of the nonlinear visco-elastic deformations of soft tissues." International journal of computer assisted radiology and surgery 6, no. 3 (2011): 297-307.